



# HHS Public Access

Author manuscript

*Biochem Biophys Res Commun.* Author manuscript; available in PMC 2017 January 15.

Published in final edited form as:

*Biochem Biophys Res Commun.* 2016 January 15; 469(3): 659–664. doi:10.1016/j.bbrc.2015.12.044.

## An adventitious interaction of filamin A with RhoGDI2(Tyr153Glu)

Mia Song<sup>1</sup>, Qianjing He<sup>1</sup>, Benjamin-Andreas Berk<sup>2</sup>, John H. Hartwig<sup>1</sup>, Thomas P. Stossel<sup>1</sup>, and Fumihiko Nakamura<sup>1</sup>

<sup>1</sup>Hematology Division, Department of Medicine, Brigham and Women's Hospital, Harvard Medical School, Boston MA USA

<sup>2</sup>Faculty of Veterinary Medicine and Faculty of Biosciences and Pharmacy, University of Leipzig, Leipzig, Germany

### Abstract

Filamin A (FLNA) is an actin filament crosslinking protein with multiple intracellular binding partners. Mechanical force exposes cryptic FLNA binding sites for some of these ligands. To identify new force-dependent binding interactions, we used a fusion construct composed of two FLNA domains, one of which was previously identified as containing a force-dependent binding site as a bait in a yeast two-hybrid system and identified the Rho dissociation inhibitor 2 (RhoGDI2) as a potential interacting partner. A RhoGDI2 truncate with 81 N-terminal amino acid residues and a phosphomimetic mutant, RhoGDI(Tyr153Glu) interacted with the FLNA construct. However, neither wild-type or full-length RhoGDI2 phosphorylated at Y153 interacted with FLNA. Our interpretation of these contradictions is that truncation and/or mutation of RhoGDI2 perturbs its conformation to expose a site that adventitiously binds FLNA and is not a bona-fide interaction. Therefore, previous studies reporting that a RhoGDI(Y153E) mutant suppresses the metastasis of human bladder cancer cells must be reinvestigated in light of artificial interaction of this point mutant with FLNA.

### Keywords

filamin; RhoGDI2; phosphorylation; src; mechanotransduction; phosphomimetic mutant

### Introduction

Filamin A (FLNA) is a homodimer, and each subunit has a N-terminal spectrin-like actin-binding domain followed by 24 immunoglobulin (Ig)-like repeats [1]. The Ig repeats are further segmented by two calpain-sensitive hinges, resulting in rod-1 (repeats 1–15), rod-2 (repeats 16–23), and dimerization domain (repeat 24) [2]. FLNA protein crosslinks actin

Corresponding: Fumihiko Nakamura, Ph.D., Translational Medicine Division, Department of Medicine, Brigham and Women's Hospital, Harvard Medical School, Boston, MA, USA, Tel: +1-617-355-9014, Fax: +1-617-355-9016, fnakamura@partners.org.

**Publisher's Disclaimer:** This is a PDF file of an unedited manuscript that has been accepted for publication. As a service to our customers we are providing this early version of the manuscript. The manuscript will undergo copyediting, typesetting, and review of the resulting proof before it is published in its final citable form. Please note that during the production process errors may be discovered which could affect the content, and all legal disclaimers that apply to the journal pertain.

filaments through the N-terminal actin-binding domain and rod-1 segment, whereas rod-2 segment is free from F-actin [3, 4]. FLNA connects F-actin to membrane proteins such as integrin and glycoproteins to stabilize plasma membrane and to transmit signals [1, 5–7]. FLNA also interacts with many signaling molecules to regulate changes in cell shape, migration, and growth and even interacts with transcription factors to regulate differentiation [8–10]. Therefore, deficiencies and mutations of FLNA in humans cause a variety of diseases, such as mental retardation, developmental malformations, and heart failure [11–13]. However, little is known about how FLNA-partner interaction is regulated. One recently demonstrated mechanism is that force-induced conformational changes of the FLNA molecule [14–16]. For example, a cytoplasmic domain of  $\beta$ -integrin binds to a cleft of the CD strands of repeat 21, which is occupied by strand A of repeat 20 in the unstressed state but becomes exposed upon application of mechanical force [14, 15]. Another example is FilGAP, a FLNA associated Rac-specific GTPase-activating protein [17], that interacts with repeat 23 when angle changes at the FLNA C-terminal spatially separate two repeat 23 domains and uncouple FilGAP from its FLNA binding sites [14, 18, 19]. Since the CD cleft of repeat 19 is also blocked with strand A of repeat 18, this repeat could potentially act as a mechano-sensing domain [20, 21].

To identify more filamin-binding proteins whose interaction is regulated by mechanical force, we performed yeast two-hybrid screening using mechano-sensing domains of FLNA as bait. We identified Rho GDP dissociation inhibitor 2 (RhoGDI2) as a potential FLNA-binding partner. RhoGDI2 is one of three RhoGDIs expressed in mammalian cells and regulates localization and activity of Rho GTPases [22, 23]. RhoGDIs act as a negative regulator of Rho GTPases and their expression levels are associated with many cancers [23, 24]. Dissociation of Rho GTPases from RhoGDIs triggers the translocation from cytoplasm to plasma membrane as well as activation of Rho GTPases [23]. Phosphorylation of RhoGDIs is one of the mechanisms that release RhoGTPases from RhoGDIs. For example, phosphorylation of Tyr-153 of RhoGDI2 by Src prevents re-binding of RhoGDIs to Rho GTPases [22]. A mutant RhoGDI with 153Tyr instead of glutamate (RhoGDI2(Y153E), predicted to mimic RhoGDI phosphorylation, suppressed metastasis of bladder cancer cells more potently than wild-type RhoGDI2 [25]. We found that the FLNA RhoGDI binding site is located adjacent to Tyr-153 and that both mutation of Tyr-153 to Glu and the opening of cryptic FLNA repeat 21 enhanced the interaction of FLNA and RhoGDI2. However, we show that full-length RhoGDI2 does not interact with FLNA and phosphorylation of Tyr-153 does not induce the interaction both *in vitro* and *in vivo*. These results imply that mutation of Tyr-153 to Glu does not mimic phosphorylation and provokes an adventitious interaction with FLNA.

## Materials and Methods

### Reagents

DMEM, fetal bovine serum, and supplements were from Invitrogen. PBS was from Corning. Plasmids for cell transfection were purified using the Qiagen HiSpeed Plasmid Midi Kit. The following reagents were purchased as indicated: OPTI-MEM (Invitrogen), monoclonal anti-Halo antibody (Promega), monoclonal anti-GFP JL-8 antibody (Clontech Laboratories),

rat anti-HA antibody (Roche), rabbit polyclonal anti-Myc antibody (Santa Cruz Biotechnology), monoclonal anti-phosphotyrosine 4G10 antibody (Millipore), glutathione Sepharose beads (GE Healthcare), goat anti-HA antibody agarose immobilized (Bethyl Laboratories), M2 anti-Flag agarose (Sigma), Super Signal West Pico Chemiluminescent Substrate (Thermo Scientific), gelatin (Sigma), Benchmark Prestained protein ladder (Invitrogen), Src kinase (Millipore).

### Anti-FLNA rabbit polyclonal antibodies

Polyclonal antibodies against FLNA was outsourced to Pacific Immunology (Ramona, CA) using human FLNA repeat 1 protein as an antigen. Human FLNA repeat 1 was chosen because its amino acid sequence is identical to that of mouse Flna repeat 1 and recombinantly expressed in *E. coli* as described below. Antibodies were affinity purified using the antigen as an affinity ligand immobilized on NHS-Sepharose (GE healthcare).

### Plasmids

The cDNA encoding RhoGDI2 and its fragments were PCR-amplified and ligated into pGEX4T-1 (GE Healthcare) by *Bam*HI/*Eco*RI sites. The cDNA encoding Halo-tag was amplified by PCR using pFN21A HaloTag® CMV Flexi® Vector (Promega) as the template, 5' primer, CATGCCATGGCAGAAATCGGTACTGG, containing a *Nco*I site, and 3' primer,

GCGGATCCTCCACCGAAATCTCCAGAGTAGACAGCCAGCGCGGATC, containing *Bam*HI site. The amplified fragments were purified, *Nco*I/*Bam*HI-digested, and ligated into *Nco*I/*Bam*HI sites of the pFASTBAC-HTb vector (Life Technologies) to generate pFASTBAC-HTb-Halo vector. cDNA encoding FLNA fragments (eg. Repeats 16–23) were amplified by PCR and ligated into pFASTBAC-HTb-Halo vector.

The His-EGFP-tagged constructs were made using pFASTBAC-HT(a or b)-EGFP plasmids [26].

pFLAG-BESN vector was constructed from pEGFP-FLNA vector ([27]) by replacing EGFP-FLNA gene with a synthetic DNA, CTAGCTAGCGCTACCGGTCGCCACCATGGACTACAAGGACGACGATGACAAAG GATCCGAATTCGTCGACGCGGCCGCTAAAC by *Nhe*I/*Not*I sites. cDNA encoding N-terminal ABD (1–153aa) was PCR amplified and ligated into pFLAG-BESN by *Bam*HI/*Eco*RI sites. cDNA encoding FLNA or FLNAdel41 ([14]) were digested with *Sal*I and *Not*I and ligated into pFLAG-ABD(1–153) by *Sal*I/*Not*I sites.

pMyc-BESN vector was constructed from pEGFP-FLNA vector ([27]) by replacing EGFP gene with a synthetic DNA, CTAGCTAGCGCTACCGGTCGCCACCATGGAGCAGAAGCTGATCAGCGAGGAGG ACCTGGGATCCGAATTCGTCGACGCGGCCGCTAAAC by *Nhe*I/*Not*I sites. cDNA encoding human RhoGDI2 was PCR-amplified using 5' primer, CGGGATCCATGACTGAAAAAGCCCCAGAG and 3' CGGAATTC AAGCGTAGTCAGGAACGTCGTATGGATATTCTGTCCACTCCTTCTTA

ATCG, and ligated into pMyc-BESN vector by BamHI/EcoRI sites to construct pMyc-RhoGDI2-HA.

pmCherry-RhoGDI2 was constructed by ligating PCR product of RhoGDI2 cDNA digested with BamHI/EcoRI into pmCherry-C1 digested with BglII/EcoRI. peGFP-FLNA wt and del41 were previously described ([14, 27]). Mutagenesis were performed using Quickchange site directed mutagenesis kit (Agilent).

### Protein expression and purification

GST-RhoGDI2 proteins were expressed at 37°C for 2 h in *E. coli* bacteria strain BL21(DE3) in the presence of 1mM Isopropyl  $\beta$ -D-1-thiogalactopyranoside (IPTG) and purified using Glutathione Sepharose beads (GE healthcare). RhoGDI2 was expressed in *E. coli* and purified as previously described [28]. His-EGFP-FLNA fragments were prepared as previously described [26]. His-Halo-FLNA fragments were expressed in sf-9 insect cells in accordance with the manufacturer's protocol (Bac-to-Bac® Baculovirus Expression Systems, Life Technologies) and purified using Ni-NTA agarose.

### Yeast Two Hybrid Screening

Yeast transformations were performed using the Frozen-EZ Yeast Transformation II kit from Zymo Research, and using the Matchmaker Gold Yeast Two-Hybrid System from Clontech Laboratories. The bait construct was pGBKT7 R19+23, which expressed the fusion protein of the GAL4-DNA-binding domain and FLNA repeats 19 and 23, and was transformed into yeast strain Y2HGold. To screen FLNA-binding protein, Mate & Plate™ Library - Normalized Universal Human (Clontech), is cloned into a pGADT7 vector and transformed into yeast strain Y187, was used. For same experiment, the prey construct was generated using pGADT7 vector, and transformed into the yeast strain Y187. The screening and assay were performed in accordance with the manufacturer's protocol.

### GST-RhoGDI2 Pull-down Assays

GST-RhoGDI2 immobilized on glutathione Sepharose beads was incubated with purified FLNA fragments tagged with Halo, His, or EGFP in buffer TBS(150)Tx (50 mM Tris-HCl, pH 7.4, 150 mM NaCl, 0.1% Triton X-100, 0.1 mM  $\beta$ -mercaptoethanol, 0.5 mM  $MgCl_2$ ). After 1h of incubation, unbound proteins were washed three times with TBS(150)Tx and bound FLNA fragments were detected by Western blotting with the appropriate antibodies.

### In vitro phosphorylation

In vitro phosphorylation activity was determined using RhoGDI2 immobilized on glutathione Sepharose beads as the substrate and purified Src kinase. One  $\mu$ g of Src kinase was used per reaction and incubated at 1 h at RT in kinase buffer (50 mM HEPES-NaOH, pH 7.5, 10 mM  $MgCl_2$ , 10 mM  $MnCl_2$ , 0.2 mM DTT, 1 mM ATP). Beads were washed three times with TBS(150)Tx, and then beads were used in pull-down assays with FLNA fragments. Bound protein was detected by Western blotting with appropriate antibodies.

## Cell Lines and Transfection

Cell lines HEK 293A (Invitrogen), Mouse embryonic fibroblast (MEF, American Type Culture Collection), and HeLa cells (American Type Culture Collection) were maintained in DMEM (Invitrogen) supplemented with 10% FBS. HEK 293A cells were transfected using Trans-IT LT1 Reagent, MEF cells were transfected using Trans-IT X2 Dynamic Delivery System, and HeLa cells were transfected using Trans-IT HeLa Monster kit; all transfection reagents were from Mirus Bio.

## Immunoprecipitation and Western Blot

HEK 293A cells were plated at 30% confluency on six-well plates and transfected with Myc-tagged RhoGDI2 plasmids using Trans-IT LT-1 transfection reagent. After 24 h, some cells were treated with activated pervanadate for 30 min [29]. After 30 min, cell lysates were collected in lysis buffer (50 mM Tris-HCl, pH 7.4, 150 mM NaCl, 0.1% Triton X-100, 1 mM EGTA, 2 mM MgCl<sub>2</sub>) supplemented with 1 mM leupeptin, 1 mM pepstatin A, 1 mM pervanadate, and 1 mM PMSF. Lysates were clarified by centrifugation at 13,000 rpm for 10 min, and the supernatant was used for immunoprecipitation. The supernatant of the cell lysate was incubated with the appropriate antibody immobilized on agarose for 1 h at 4 C. Beads were collected by centrifugation at 1K rpm for 2 min and washed three times with TBS(150)Tx. Proteins were eluted by adding 3X SDS sample buffer and heating to 95 C for 5 min. Samples were subject to SDS-PAGE and then Western blotting with the appropriate antibodies.

## Microscopy

Eight-well chamber glass slides from LAB-TEK were treated with gelatin before plating MEF cells. Transfected cells were imaged using a spinning-disk confocal microscope: spinning-disk head (CSU-X1, Yokogawa), microscope stand (IX81, Olympus), 488nm and 561nm laser combiner (ALC, Andor Technology), EMCCD camera (iXon 897, Andor Technology), laser based focusing system (ZDC1, Olympus), objective (60×/1.2 NA UPLSAPO 60XW water immersion lens, Olympus), image acquisition software (MetaMorph 7.7.7.0, Molecular Devices), stage top humidified chamber (INU-ZILCS-F1, Tokai Hit), whole microscope 37°C chamber (custom designed by HMS Cell Biology machine shop), Semrock barrier filters (525/40, 607/36), Semrock dichroic mirror (405/488/568/647). Wavelengths of the excitation laser beam were 488 and 561 nm and fluorescence for mEGFP and mCherry was detected using 488/568 nm Yokogawa emission filter (Em01-R488/568-15, Semrock). Images were collected using the maximum field of view with 512 × 512 image size. Some cells were imaged after permeabilization with 0.75% TritonX-100 in PHEM (60 mM Pipes, 25 mM Hepes, 10 mM EGTA, 2 mM MgCl<sub>2</sub>, pH 6.9) buffer containing 5 μM phalloidin and 3.7% of formaldehyde for 2 min and washed with PHEM containing 3.7% of formaldehyde.

## Data presentation

All experiments were repeated at least in triplicate and representative results from a single experiment are shown in the figures.

## Results and Discussion

### Identification of RhoGDI2 as a potential FLNA-binding partner

The well-defined FLNA binding partner sites on repeats 19 and 23 were fused and used as bait for a yeast two-hybrid screen of the human universal cDNA library (Figure 1A). The interaction of these sites with their partners is regulated by avidity interactions, as tight binding requires each filamin molecule to bind two identical sites on its dimeric partner protein, either GP1ba or FilGAP [14], respectively. RhoGDI2 was identified as a potential FLNA partner in this screen.

We obtained cDNA encoding amino acids 82–201 of RhoGDI2 (Figure 1B). Although no interaction was detected with full-length RhoGDI2 in yeast two-hybrid (Figure 1B), RhoGDI2 fused to GST could pull down a FLNA construct composed of repeats 19–23 (Figure 1C). We speculated that incomplete folding of RhoGDI2 protein in *E. coli* or deletion of the N-terminal 81 amino acids exposed an intrinsic FLNA-binding site. Since post-translational modification could induce a conformational change of RhoGDI2 and expose such binding site, we pursued this possibility.

### Mapping of FLNA/RhoGDI2 interaction sites

Using Halo-tagged FLNA fragments, we found that GST-RhoGDI2 pulls down FLNA constructs composed of 8–15, 16–23, but not 1–8 repeats (Supplementary Figure 1A). To narrow down the binding site, we incubated individual EGFP-tagged FLNA repeats with GST-RhoGDI2 coated beads (Supplementary Figure 1B) and found that the beads pull down many different FLNA repeats, binding best to repeats 9, 19, 23, and hinge2–24b and less well to repeats 17 and 21. These findings suggest that RhoGDI2 interacts with the CD cleft of these repeats except for hinge2–24 because they are structurally similar and share a conserved ligand-binding site [26, 30].

To map the FLNA-binding site on RhoGDI2, a purified Halo-FLNA19–23 construct was incubated with GST-tagged RhoGDI2 fragments (Supplementary Figure 1C). The FLNA-binding site was delimited to residues 120–146 of RhoGDI2 that forms anti-parallel  $\beta$ -strands that face GDP-Rac. (Supplementary Figure 1D).

### Effect of phosphomimetic mutation on RhoGDI2 binding to FLNA

Studies have shown that Src kinase primarily phosphorylates RhoGDI2 at Tyr153 to regulate its interaction with Rho GTPases [22, 25]. Mutation of Tyr153 to glutamate prevents this interaction, and causes this mutant RhoGDI2 (Y1532E) to localize at membrane ruffles [22]. In expression studies, the mutant RhoGDI2 (Y1532E) more potently suppresses metastasis of bladder cancer cells than does the wild-type RhoGDI2 [25]. Since Tyr153 is located near the FLNA-binding site, we tested the effect of the Tyr153 to glutamate mutation on FLNA-binding (Figure 2). We co-expressed wild-type or mutant Myc-RhoGDI2-HA with Flag-tagged FLNA or a FLNA del41 variant in HeLa cells. FLNA del41 removes the auto-inhibitory domain (strand A) of repeat 20 from repeat 21 constitutively revealing its cryptic binding site [31–33] (Figure 2A). Wild-type RhoGDI2 failed to co-immunoprecipitate either form of FLNA, whereas mutant RhoGDI2(Y153E)

collected FLNA even though the expression level of mutant RhoGDI2(Y153E) was lower than that of wild-type. Exposure of the binding site of repeat 21 in FLNA del41 increased the interaction, demonstrating that RhoGDI2(Y153E) interacts with the cleft formed by the CD  $\beta$ -strands of repeat 21. Yeast two-hybrid assay also confirmed that the interaction between RhoGDI2(Y153E) and FLNA repeats 19+23 was through their CD clefts as mutations in certain critical amino acids of the CD  $\beta$ -strands within the ligand binding site disrupted this interaction (Figure 2B). Consistent with this biochemical data, mutant RhoGDI2(Y153E) was co-localized with FLNA in the detergent insoluble cytoskeleton of cells, whereas wild-type RhoGDI2 was primarily released into the soluble protein phase (Supplementary Figure 2).

### Intact FLNA and phospho-RhoGDI2 do not interact

The colocalization of RhoGDI2(Y153E) and FLNA in the cytoskeleton suggested that phosphorylation of Tyr153 in RhoGDI2 promotes its interaction with FLNA. Hence, we phosphorylated purified recombinant GST-RhoGDI2 with purified Src kinase *in vitro* and incubated it with Halo-FLNA19–23 del41 (Figure 3A). Although GST-RhoGDI2 was phosphorylated, detected by anti-phosphoTyr antibody blotting, it did not alter its the interaction with FLNA19–23 del41 (Figure 3A). To specifically test the 153 site, we co-expressed Flag-FLNA del41 with wild-type or mutant Myc-RhoGDI2-HA (wt, Y153E, or Y153F) in HEK cells and treated them with pervanadate to inhibit tyrosine phosphatase activity (Figure 3B). Pervanadate treatment increased the amount of Tyr153 phosphorylation detected in RhoGDI2, no interaction between phospho-RhoGDI2 and FLNA del41 was detected, although both the mutant RhoGDI2 (Y153E and Y153F) co-immunoprecipitated with Flag-FLNA del41 (Figure 3B). In an effort to further enhance the phosphorylation of Tyr153, we co-expressed Myc-RhoGDI2-HA with constitutively active Src kinase (Y530F) and treated the cells again with the phosphatase inhibitor (Figure 3C). Mutation of Tyr153 to Glu dramatically reduced phosphorylation, indicating that Tyr153 is indeed phosphorylated in cells but did not induce binding to FLNA (Figure 3C).

Our results demonstrated that mutation of Tyr153 to Glu in RhoGDI not only does not mimic the effects of RhoGDI phosphorylation but also induces an extrinsic interaction with FLNA. The results also showed that this adventitious interaction is mediated through a hidden FLNA-binding site that is exposed by improper folding of RhoGDI2 due to the truncation of its N-terminal 81 amino acids, overexpression in *E.coli*, and point mutation at Tyr153 to Glu or Phe. This result is not the first example demonstrating that the mutation from Tyr to Glu does not mimic phosphorylation [34]. These results clearly indicate that such point mutation results need to be carefully validated before drawing physiologic inferences. However, the presented data cannot exclude the possibility that other physiological modifications on RhoGDI drive a conformational change to make the interaction possible.

A previous study suggested cautious use of Src kinase inhibitors for cancer therapy because RhoGDI2(Y153E) was a more potent suppressor of lung metastasis of bladder cancer cell lines than wild-type RhoGDI2, and inhibition of Src kinase may relieve metastasis suppression in tumor cells [25]. Since FLNA-binding partner interactions regulate cell

adhesion, spreading, and migration [1, 7], the suppression effect of RhoGDI2(Y153E) may be due to nonspecific perturbations of FLNA-mediated signaling, and inhibition of Src kinase may not necessarily provoke metastasis through RhoGDI2.

## Supplementary Material

Refer to Web version on PubMed Central for supplementary material.

## Acknowledgments

The authors thank the HUSEC Seed Fund for Interdisciplinary Science and a National Institutes of Health grant (HL19749).

## References

1. Stossel TP, Condeelis J, Cooley L, Hartwig JH, Noegel A, Schleicher M, Shapiro SS. Filamins as integrators of cell mechanics and signalling. *Nature reviews. Molecular cell biology*. 2001; 2:138–145. [PubMed: 11252955]
2. Gorlin JB, Yamin R, Egan S, Stewart M, Stossel TP, Kwiatkowski DJ, Hartwig JH. Human endothelial actin-binding protein (ABP-280, nonmuscle filamin): a molecular leaf spring. *J Cell Biol*. 1990; 111:1089–1105. [PubMed: 2391361]
3. Nakamura F, Osborn TM, Hartemink CA, Hartwig JH, Stossel TP. Structural basis of filamin A functions. *J Cell Biol*. 2007; 179:1011–1025. [PubMed: 18056414]
4. Suphamongmee W, Nakamura F, Hartwig JH, Lehman W. Electron microscopy and 3D reconstruction reveals filamin Ig domain binding to F-actin. *Journal of molecular biology*. 2012; 424:248–256. [PubMed: 23041423]
5. Feng S, Resendiz JC, Lu X, Kroll MH. Filamin A binding to the cytoplasmic tail of glycoprotein Ibalph $\alpha$  regulates von Willebrand factor-induced platelet activation. *Blood*. 2003; 102:2122–2129. [PubMed: 12791664]
6. Cunningham CC, Gorlin JB, Kwiatkowski DJ, Hartwig JH, Janmey PA, Byers HR, Stossel TP. Actin-binding protein requirement for cortical stability and efficient locomotion. *Science (New York, N.Y.)*. 1992; 255:325–327.
7. Nakamura F, Stossel TP, Hartwig JH. The filamins: organizers of cell structure and function. *Cell adhesion & migration*. 2011; 5:160–169. [PubMed: 21169733]
8. Zhou AX, Hartwig JH, Akyurek LM. Filamins in cell signaling, transcription and organ development. *Trends in cell biology*. 2010; 20:113–123. [PubMed: 20061151]
9. Johnson K, Zhu S, Tremblay MS, Payette JN, Wang J, Bouchez LC, Meeusen S, Althage A, Cho CY, Wu X, Schultz PG. A stem cell-based approach to cartilage repair. *Science (New York, N.Y.)*. 2012; 336:717–721.
10. Mondal G, Rowley M, Guidugli L, Wu J, Pankratz VS, Couch FJ. BRCA2 localization to the midbody by filamin A regulates cep55 signaling and completion of cytokinesis. *Developmental cell*. 2012; 23:137–152. [PubMed: 22771033]
11. Robertson SP. Molecular pathology of filamin A: diverse phenotypes, many functions. *Clinical dysmorphology*. 2004; 13:123–131. [PubMed: 15194946]
12. Yue J, Huhn S, Shen Z. Complex roles of filamin-A mediated cytoskeleton network in cancer progression. *Cell & bioscience*. 2013; 3:7. [PubMed: 23388158]
13. Zhou X, Boren J, Akyurek LM. Filamins in cardiovascular development. *Trends in cardiovascular medicine*. 2007; 17:222–229. [PubMed: 17936203]
14. Ehrlicher AJ, Nakamura F, Hartwig JH, Weitz DA, Stossel TP. Mechanical strain in actin networks regulates FilGAP and integrin binding to filamin A. *Nature*. 2011; 478:260–263. [PubMed: 21926999]



15. Rognoni L, Stigler J, Pelz B, Ylanne J, Rief M. Dynamic force sensing of filamin revealed in single-molecule experiments. *Proc Natl Acad Sci U S A*. 2012; 109:19679–19684. [PubMed: 23150587]
16. Razinia Z, Makela T, Ylanne J, Calderwood DA. Filamins in mechanosensing and signaling. *Annual review of biophysics*. 2012; 41:227–246.
17. Ohta Y, Hartwig JH, Stossel TP. FilGAP, a Rho- and ROCK-regulated GAP for Rac binds filamin A to control actin remodelling. *Nature cell biology*. 2006; 8:803–814. [PubMed: 16862148]
18. Nakamura F, Heikkinen O, Pentikainen OT, Osborn TM, Kasza KE, Weitz DA, Kupiainen O, Permi P, Kilpelainen I, Ylanne J, Hartwig JH, Stossel TP. Molecular basis of filamin A-FilGAP interaction and its impairment in congenital disorders associated with filamin A mutations. *PLoS ONE*. 2009; 4:e4928. [PubMed: 19293932]
19. Nakamura F. FilGAP and its close relatives: a mediator of Rho-Rac antagonism that regulates cell morphology and migration. *The Biochemical journal*. 2013; 453:17–25. [PubMed: 23763313]
20. Ruskamo S, Gilbert R, Hofmann G, Jiang P, Campbell ID, Ylanne J, Pentikainen U. The C-terminal rod 2 fragment of filamin A forms a compact structure that can be extended. *The Biochemical journal*. 2012; 446:261–269. [PubMed: 22676060]
21. Tossavainen H, Koskela O, Jiang P, Ylanne J, Campbell ID, Kilpelainen I, Permi P. Model of a six immunoglobulin-like domain fragment of filamin A (16–21) built using residual dipolar couplings. *Journal of the American Chemical Society*. 2012; 134:6660–6672. [PubMed: 22452512]
22. DerMardirossian C, Rocklin G, Seo JY, Bokoch GM. Phosphorylation of RhoGDI by Src regulates Rho GTPase binding and cytosol-membrane cycling. *Molecular biology of the cell*. 2006; 17:4760–4768. [PubMed: 16943322]
23. Garcia-Mata R, Boulter E, Burridge K. The 'invisible hand': regulation of RHO GTPases by RHOGDIs. *Nature reviews. Molecular cell biology*. 2011; 12:493–504. [PubMed: 21779026]
24. Griner EM, Theodorescu D. The faces and friends of RhoGDI2. *Cancer metastasis reviews*. 2012; 31:519–528. [PubMed: 22718398]
25. Wu Y, Moissoglu K, Wang H, Wang X, Frierson HF, Schwartz MA, Theodorescu D. Src phosphorylation of RhoGDI2 regulates its metastasis suppressor function. *Proc Natl Acad Sci U S A*. 2009; 106:5807–5812. [PubMed: 19321744]
26. Playford MP, Nurminen E, Pentikainen OT, Milgram SL, Hartwig JH, Stossel TP, Nakamura F. Cystic fibrosis transmembrane conductance regulator interacts with multiple immunoglobulin domains of filamin A. *The Journal of biological chemistry*. 2010; 285:17156–17165. [PubMed: 20351098]
27. Nakamura F, Pudas R, Heikkinen O, Permi P, Kilpelainen I, Munday AD, Hartwig JH, Stossel TP, Ylanne J. The structure of the GPIb-filamin A complex. *Blood*. 2006; 107:1925–1932. [PubMed: 16293600]
28. Golovanov AP, Chuang TH, DerMardirossian C, Barsukov I, Hawkins D, Badii R, Bokoch GM, Lian LY, Roberts GC. Structure-activity relationships in flexible protein domains: regulation of rho GTPases by RhoGDI and D4 GDI. *Journal of molecular biology*. 2001; 305:121–135. [PubMed: 11114252]
29. Pumiglia KM, Lau LF, Huang CK, Burroughs S, Feinstein MB. Activation of signal transduction in platelets by the tyrosine phosphatase inhibitor pervanadate (vanadyl hydroperoxide). *The Biochemical journal*. 1992; 286(Pt 2):441–449. [PubMed: 1530576]
30. Ithychanda SS, Hsu D, Li H, Yan L, Liu DD, Das M, Plow EF, Qin J. Identification and characterization of multiple similar ligand-binding repeats in filamin: implication on filamin-mediated receptor clustering and cross-talk. *The Journal of biological chemistry*. 2009; 284:35113–35121. [PubMed: 19828450]
31. van der Flier A, Kuikman I, Kramer D, Geerts D, Kreft M, Takafuta T, Shapiro SS, Sonnenberg A. Different splice variants of filamin-B affect myogenesis, subcellular distribution, and determine binding to integrin [beta] subunits. *J Cell Biol*. 2002; 156:361–376. [PubMed: 11807098]
32. Lad Y, Kiema T, Jiang P, Pentikainen OT, Coles CH, Campbell ID, Calderwood DA, Ylanne J. Structure of three tandem filamin domains reveals auto-inhibition of ligand binding. *The EMBO journal*. 2007; 26:3993–4004. [PubMed: 17690686]

33. Pentikainen U, Jiang P, Takala H, Ruskamo S, Campbell ID, Ylanne J. Assembly of a filamin four-domain fragment and the influence of splicing variant-1 on the structure. *The Journal of biological chemistry*. 2011; 286:26921–26930. [PubMed: 21636571]
34. Anthis NJ, Haling JR, Oxley CL, Memo M, Wegener KL, Lim CJ, Ginsberg MH, Campbell ID. Beta integrin tyrosine phosphorylation is a conserved mechanism for regulating talin-induced integrin activation. *The Journal of biological chemistry*. 2009; 284:36700–36710. [PubMed: 19843520]
35. Kiema T, Lad Y, Jiang P, Oxley CL, Baldassarre M, Wegener KL, Campbell ID, Ylanne J, Calderwood DA. The molecular basis of filamin binding to integrins and competition with talin. *Mol Cell*. 2006; 21:337–347. [PubMed: 16455489]

**Highlights**

- RhoGDI2 is identified as a potential filamin A (FLNA)-binding partner.
- Phosphomimetic mutant, RhoGDI2(Tyr153Glu) interacts with FLNA.
- RhoGDI2 phosphorylated (Tyr153) by src kinase does not interact with FLNA.
- Mutation of Tyr-153 to Glu of RhoGDI2 does not mimic phosphorylation.
- RhoGDI2(Tyr153Glu) provokes an adventitious interaction with FLNA.

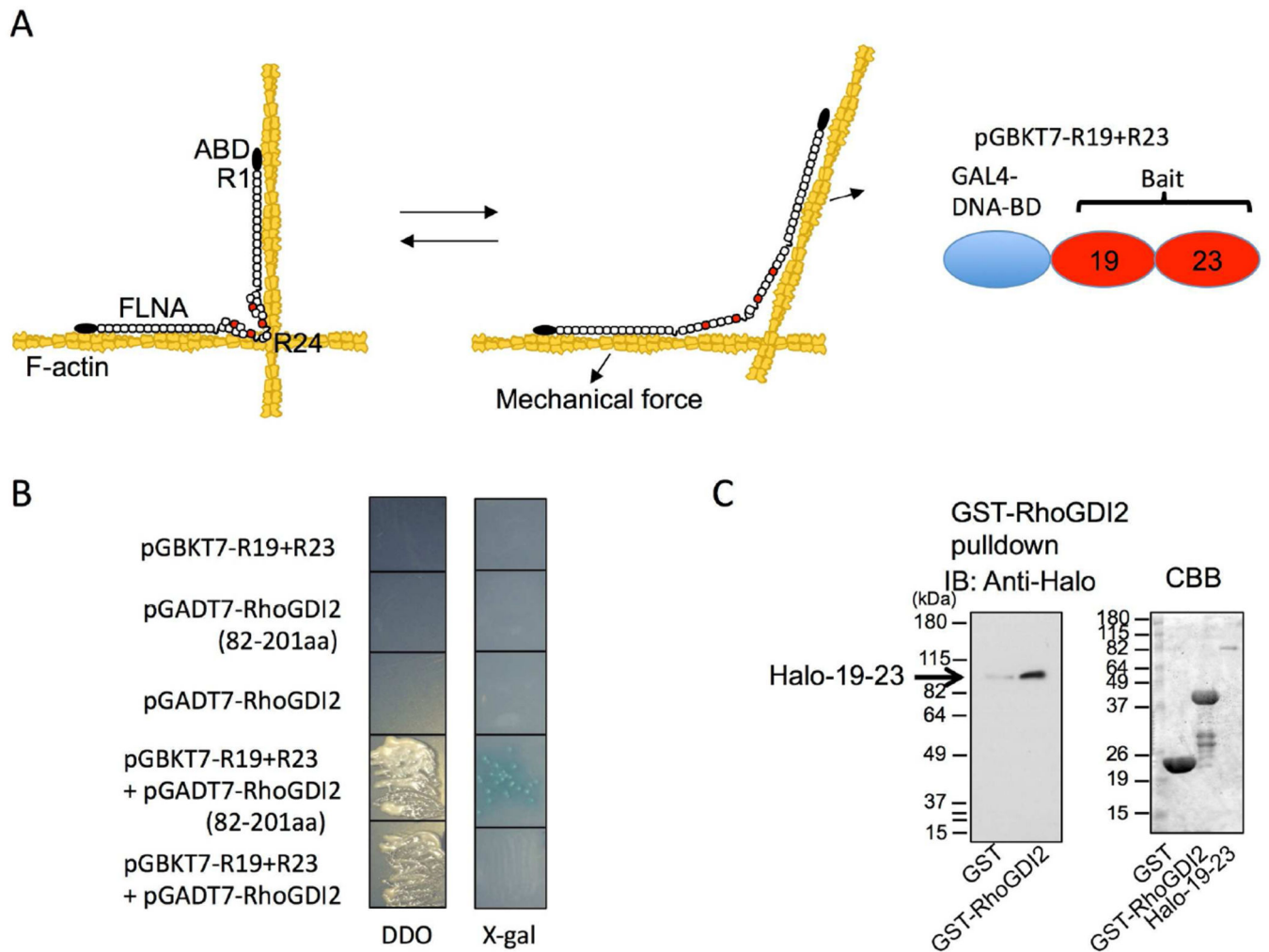


**Figure 1. Identification of RhoGDI2 as a potential FLNA binding partner**

(A) A scheme of how mechanical force induces conformational changes of FLNA molecule. N-terminal actin-binding domain (ABD). Immunoglobulin-like repeat 1 (R1). R19 and R23 are indicated in red. The right panel shows a bait construct pGBKT7 R19+23, which expresses the fusion protein of the GAL4-DNA-binding domain and FLNA repeats 19 and 23. (B) Interaction of RhoGDI2 (82–201aa) with FLNA19+23 by yeast two-hybrid assay. Photo images displayed yeast colony growth (DDO: double dropout) and  $\beta$ -galactosidase staining (X-gal). Expression of a bait or prey alone did not yield growth. Expression of FLNA19+23 with full-length RhoGDI2 resulted in growth on DDO plate but no color development or growth on X-gal plate. (C) GST-RhoGDI2 pulldown assay. Halo-tagged FLNA19–23 was pulled down with GST-RhoGDI2 immobilized on glutathione-Sepharose beads. Coomassie Brilliant Blue (CBB) stained gel shows purified proteins used.

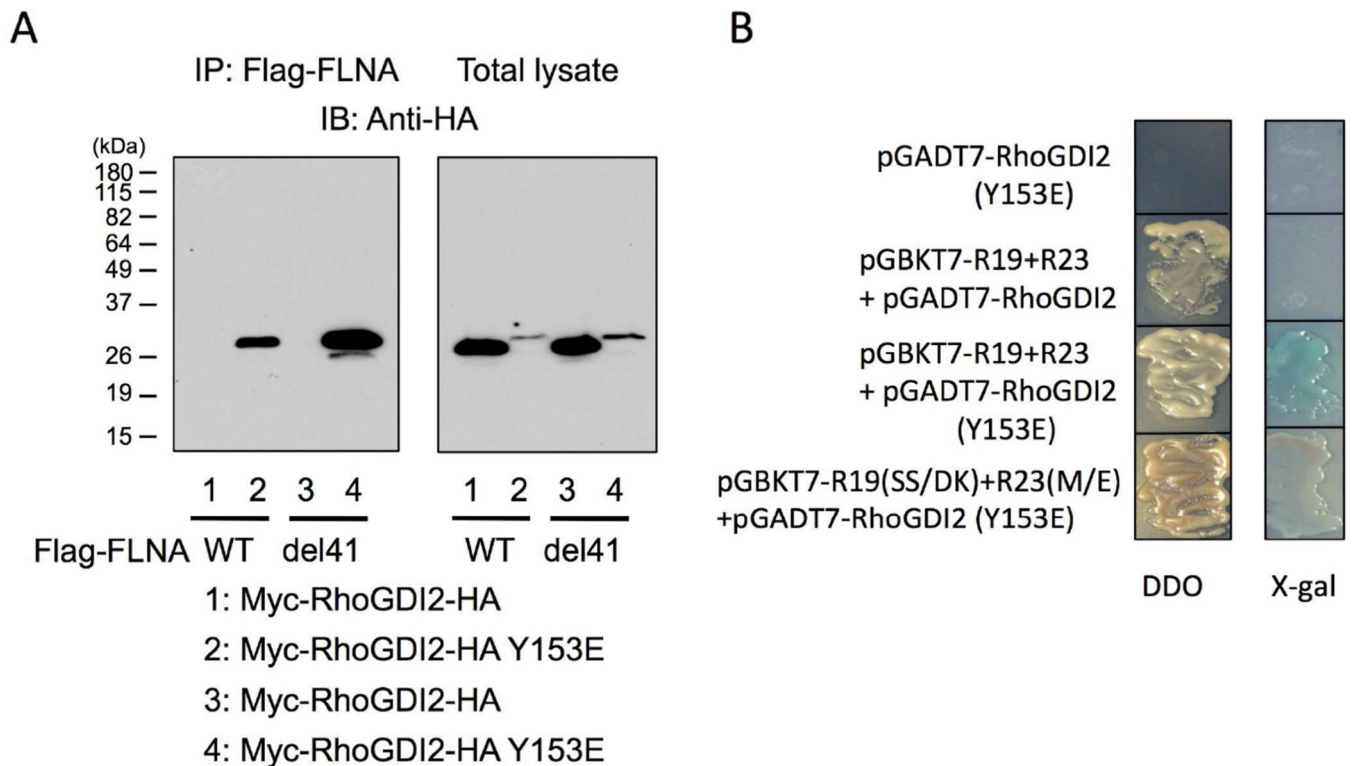


**Figure 2. A point mutation of Tyr153 RhoGDI2 to Glu induces binding to full-length FLNA**  
(A) Interaction of RhoGDI2(Y153E) with full-length FLNA *in vivo*. Wild-type (WT) or mutant (Y153E) Myc-RhoGDI2-HA was co-expressed with Flag-FLNA (WT or del41) in HEK-293 cells. Flag-FLNA was pulled down with anti-Flag antibody coated beads and bound protein was detected with anti-HA antibody. (B) Yeast two-hybrid assay of mutant RhoGDI2 (Y153E) and FLNA19+23. It was previously shown that point mutations of the C strand of repeat 19 (SS/DK: S2081D and S2083K) disrupt binding to  $\beta$ -integrin [35] and point mutation of the D strand of repeat 23 (M/E: M2474E) disrupts binding to FilGAP [18]. Photo images displayed yeast colony growth (DDO) and  $\beta$ -galactosidase staining (X-gal). Expression of RhoGDI2(Y153E) alone did not yield growth. Expression of mutant FLNA19+23 (SS/DK, M/E) with mutant RhoGDI2 (Y153E) resulted in growth but not color development.

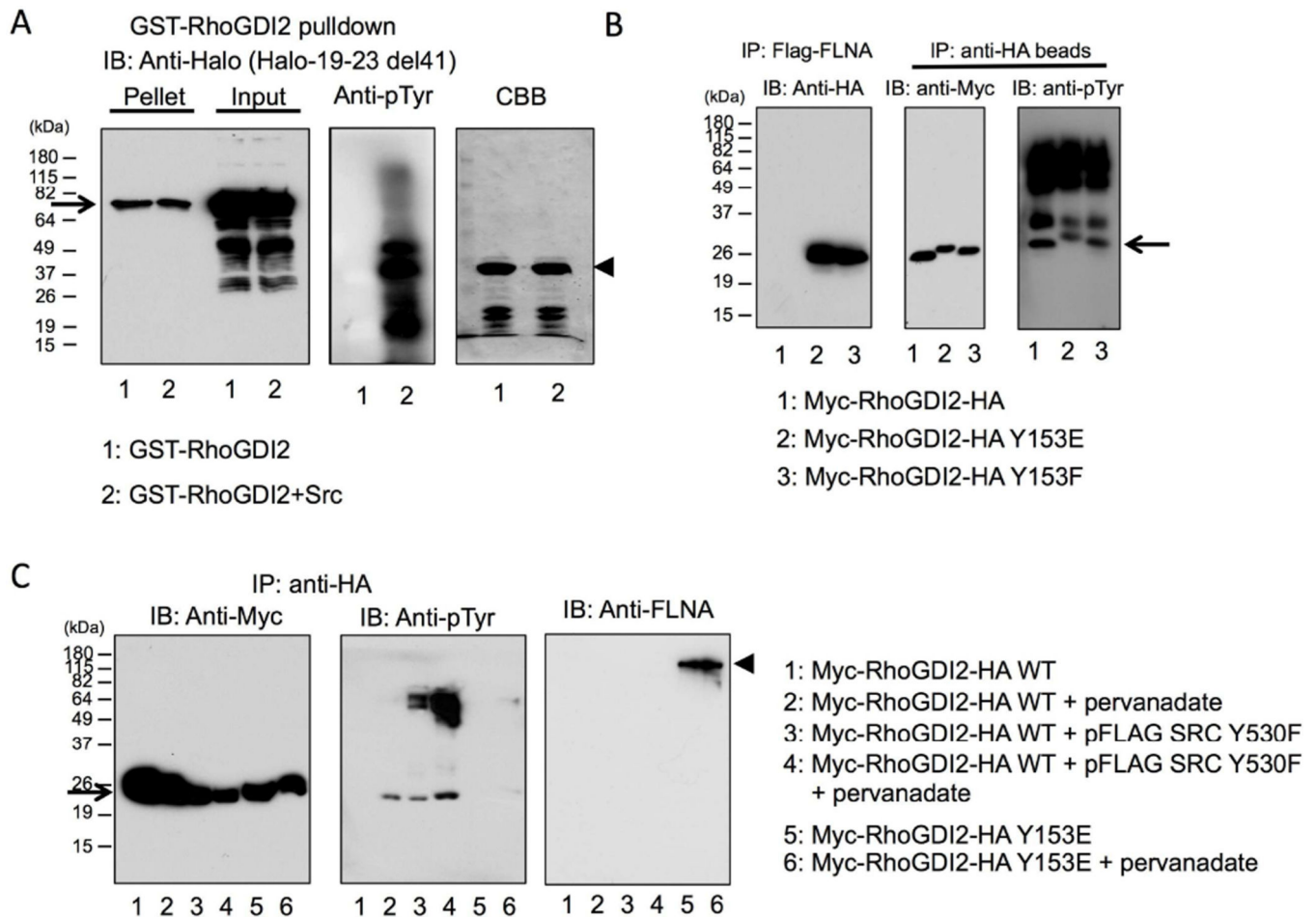


**Figure 3. Effect of phosphorylation of RhoGDI2 by Src kinase on FLNA-binding**

(A) Phosphorylation of GST-RhoGDI2 by purified Src kinase *in vitro* does not affect the interaction with FLNA. GST-RhoGDI2 immobilized on glutathione-Sepharose was phosphorylated by Src kinase, washed, and incubated with Halo-FLNA 19–23 del41. Bound FLNA was detected by anti-Halo antibody (left panel, arrow). Phosphorylation of GST-RhoGDI2 was detected by anti-phosphoTyr antibody (middle panel). CBB stained gel shows purified GST-RhoGDI2 (right panel, arrowhead). (B) Full-length FLNA does not interact with phosphorylated RhoGDI2 in cells. Wild-type or mutant Myc-RhoGDI2-HA were co-expressed with Flag-FLNA del 41 in HEK-293 cells and treated with pervanadate for 30 min. Flag-FLNA del41 was pulled down with anti-Flag antibody-coated beads and bound protein was detected by immunoblotting using anti-HA antibody (left panel). Myc-RhoGDI2-HA transfected in cells were immunoprecipitated with anti-HA antibody-coated beads and precipitates were detected with anti-myc antibody (middle panel) and anti-phosphoTyr antibody (right panel). Note that wild-type RhoGDI2 is more phosphorylated than mutant RhoGDI2 (Y153E and Y153F), indicating that Tyr-153 is phosphorylated in cells. (C) Enhanced phosphorylation of RhoGDI2 by constitutively active Src kinase. Myc-RhoGDI2-HA WT and constitutively active Src(Y530F) kinase were co-expressed in HEK-293 cells and immunoprecipitated with anti-HA antibody-coated beads. Some cells were treated with pervanadate before immunoprecipitation.

Precipitated Myc-RhoGDI2-HA were detected with anti-myc antibody (left panel, arrow) and phosphorylation was detected with anti-phosphoTyr antibody (middle panel). Co-precipitated endogenous FLNA was detected by anti-FLNA antibody (right blot, arrowhead). Note that both co-expression of Src and treatment with pervanadate greatly enhanced phosphorylation of RhoGDI2 at Tyr-153, but failed to induce FLNA-binding.

Author Manuscript

Author Manuscript

Author Manuscript

Author Manuscript